RATE DETERMINING STEP IN THE GASEOUS REDUCTION OF PURE AND DOPED IRON OXIDES

Abdel-Hady El-Geassy
Central Metallurgical Research and Development Institute, Egypt

ABSTRACT

Pure wüstite, W1 ($Fe_{0.941}O$) and SiO_2-doped wüstite W2 micropellets (SiO_2-$Fe_{0.947}O$) were prepared by the non-isothermal reduction of Fe_2O_3 and 2.1 mass% SiO_2-Fe_2O_3 sintered compacts. The wüstite micro-pellets (250-150 µm) were characterized by XRD, specific surface area and their structures were examined with optical and scanning electron microscopes supported with Energy Dispersive X-ray analysis (EDX). W1 and W2 micropellets were isothermally reduced to metallic iron at 900-1100°C with H_2, CO and their mixtures. The O_2-weight loss resulted from the reduction process was continuously recorded as a function of time. The influences of gas composition, temperature and total gas pressure (0.1 up to 1.0 atm) on the reduction rate were intensively studied and correlated to predict the corresponding reduction mechanism. The highest reduction rate (dr/dt) was obtained in H_2 and the lowest was in CO at their initial reduction stages. In H_2/CO gas mixture, the rate did not vary with gas composition in a simple manner. At final reduction stages, unlike in CO, a rate minimum was detected at 900-950°C in H_2 and H2-rich gas mixtures which was attributed to α-γ Fe transformation. The presence of SiO_2 enhanced the reduction in CO and CO/H_2 mixtures. In H_2, a significant slowing down in the rate at later stages was noticed due to the presence of hardly reducible fayalite phase (Fe_2SiO_4). Iron carbide was identified in samples reduced by CO-containing gas mixtures. An incubation period was detected at lower temperature and increased with the decrease in PCO. The reduction mechanism was also proposed.

INTRODUCTON

Iron ores are converted into metallic iron in the blast furnace, which accounts about 95% of the world production. Direct reduction and smelting reduction processes are producing the balance. In most of direct reduction plants, iron oxides are reduced with reformed natural gas (H_2/CO mixtures). DRI has gained a wide acceptance in electric arc furnace steelmaking process, due to the decline in the availability of high quality scrap. In foundry industries, sponge iron is used in production of gray and ductile cast iron. The reduction of iron ores is a complex process involving a great number of physical and chemical variables. The structure and morphology of the intermediate oxides (magnetite and/or wüstite) are far from starting materials and have a great influence on the reduction kinetics. The presence of impurities usually associated with iron ores such as SiO_2, CaO, MgO, Al_2O_3, MnO, etc., further complicates the reduction process [1, 2, 3]. Most of previous studies were dealt with one step reduction process ($Fe_2O_3 \rightarrow Fe$), and scant attentions were given to the intermediate reduction steps. Recent publications [4, 5, 6, 7, 8] paid higher attention to the reduction kinetics and mechanism of the intermediate steps. The mechanism of reduction with CO is different from that with H_2 and with H_2/CO gas mixtures [9]. The presence of impurities promotes nucleation and grain growth of magnetite. The wüstite-iron transformation step is kinetically regarded as the most significant step, which controls the overall reduction process and different reduction models were proposed [10, 11]. Thus, the present investigation concerns with the reduction kinetics and mechanism of wüstite pure and SiO_2 doped-wüstite micropellets at different reduction conditions.

METHODOLOGY

Chemically pure Fe_2O_3 and Fe_2O_3 doped with 2.1% SiO_2 compacts sintered at 1350°C for 3hrs were prepared. Compacts were then partially reduced to wüstite in 60%CO-40%CO_2 gas mixture at 1000°C till a constant weight loss was attained after which they cooled down in O_2-free Ar gas to room temperature. The sintered compacts were crushed and 250+150μm size fraction was collected. The chemical formulae of pure wüstite is $Fe_{0.941}O$, while that for and SiO_2 doped-wüstite is $Fe_{0.947}O$, which reported herein after as W1 and W2 respectively. The specific surface area of W1 and W2 are 0.0520 and 0.1218 m^2/g respectively. The SEM photomicrographs of W1 and W2 are shown in Figure 1. It shows that, while W1 is dense and exhibited facetted plates, W2 is porous and contains macropores due to the presence of fayalite ($2FeO.SiO_2$) phase which counteracts recrystallization and sintering of micrograins.

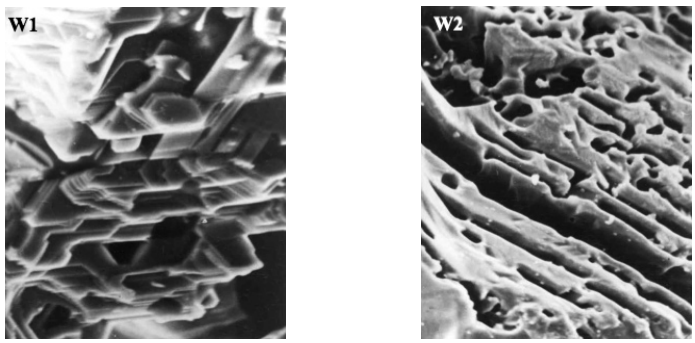

Figure 1: SEM Photomicrograph of W1 and W2 micropellets (5000X)

W1 and W2 micropellets were isothermally reduced with purified H_2, CO and their mixture at 900-1100°C. The O_2-weight loss resulted from The reduction of wüstite to iron is continuously recorded as a function of time using a TGA analysis technique [12, 13]. The reduction was carried out at different total gas pressures (0.1-1.0 atm.). Partially and completely reduced samples are examined with optical (LM) and scanning electron microscopes (SEM). X-ray phase identification, total carbon analysis and surface area measurements (BET) techniques are also applied.

RESULTS AND DISCUSSION

Reduction Kinetics

The typical reduction curves of W1 and W2 micropellets at 900-1100°C with H_2 and/or CO were given elsewhere [18, 19]. Figure 2 (a,b) shows an example for the reduction of W1 and W2 micropellets 1000°C with H_2 and/or CO gas mixtures respectively. They show clearly that the presence of SiO_2 has a great influence in the behaiour during reduction which is also gas dependant.

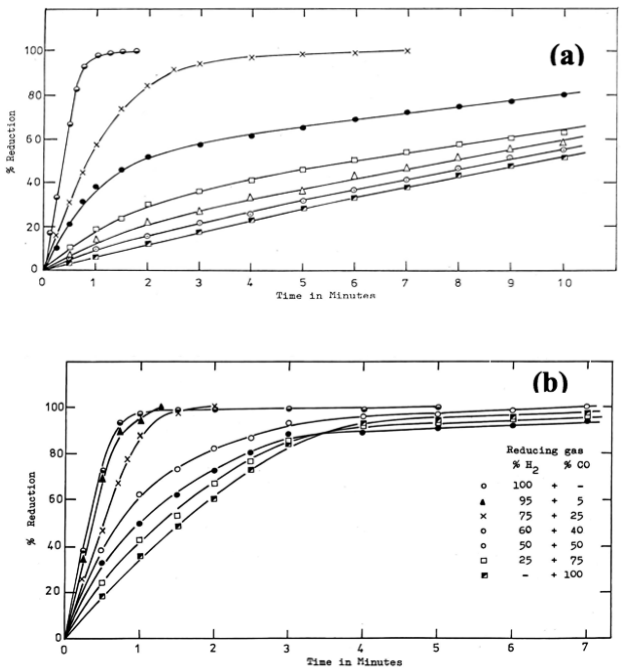

Figure 2: Typical Reduction curves of W1 (a) and W2 (b) at 1000°C

The influence of total gas pressure of CO (P_{CO} = 0.1-1.0 atm) on the reduction behaviour of W1 micropellets at 1000°C is illustrated in Figure 3.

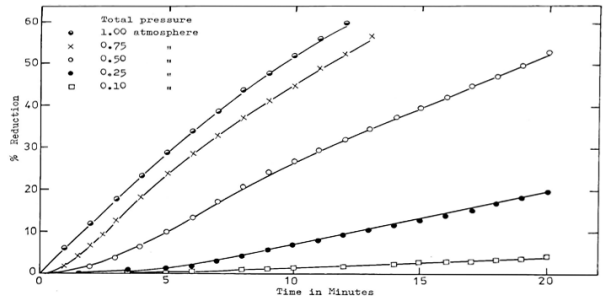

Figure 3: Influence of CO gas pressure on the reduction of W1 at 1000°C

It can be observed that, unlike the reduction of W2, the reduction of W1 with CO, at lower P_{CO} pressures (< 0.5 atm.) clearly shows the presence of an incubation period and the reduction curve exhibited three distinct reduction zones as illustrated the diagram given in Figure 4.

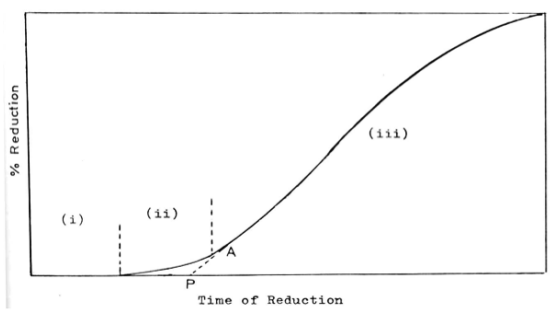

Figure 4: Schematic diagram for the reduction with CO at P_{CO}< 0.5 atm

It can be observed that, unlike the reduction of W2 with CO, the reduction of W1 with CO, at lower P_{CO} pressures (< 0.5 atm.), exhibited three distinct reduction zones as illustrated in Figure 7; i) incubation period, where no measurable weight loss could detected, ii) induction period, where the rate of reduction increases, and iii) deceleration rate period, where the rate decreases gradually with time up to the end of reduction process.

To highlight this phenomena more clearly, the relationship between the rate of reduction (dr/dt) at the initial stages(5% extents) and the corresponding reducing gas composition is given in Figure 5.

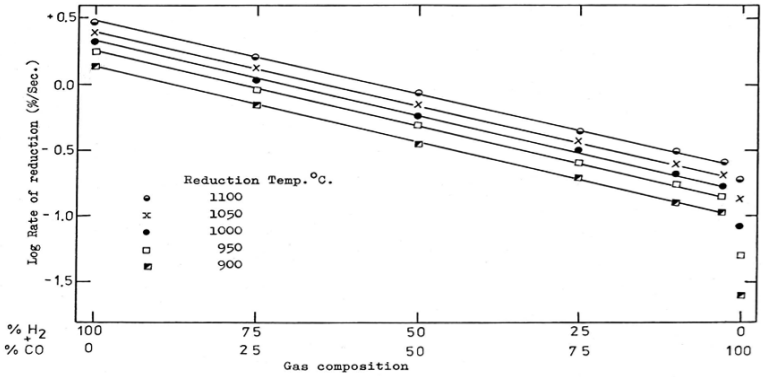

Figure 5: Influence of reducing gas composition on the reduction rate of W1

The results showed that the rate of reduction gradually decreases with the increase in CO content in the gas mixture. In pure CO, an abrupt decrease in the rate was observed and this decrease decreases with rise in temperatures. This slowing down effect in the rate was eliminated in presence of 2.5%H_2 in H_2/CO. The influence of H_2 addition to CO on the rate of reduction (dr/dt) of W1 micropellets is shown in Figure 6.

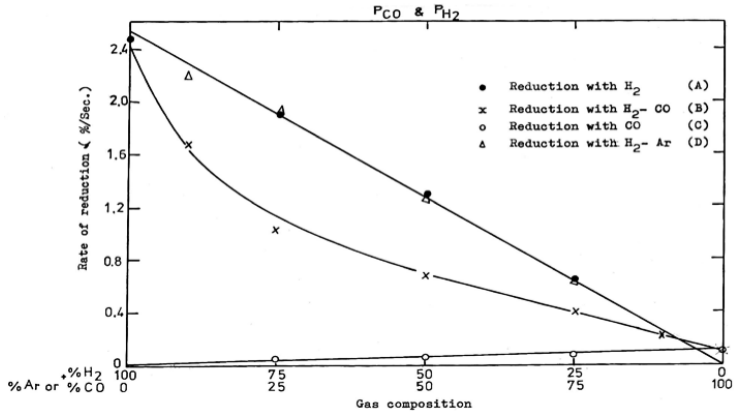

Figure 6: Variation between dr/dt for W1 at 1000°C with gases

In this experiment, the reduction of W1 was carried out with H_2,CO, H_2/CO and H_2/Ar. For the reduction with H_2 or with CO, a linear relationship between the rate of reduction, (*R), and the H_2 content in the mixture, X_{H2}, followed the relationship;

$$\ln (^*R)_{mixture} = - A\ X_{H2} + \ln (^*R)_{H2} \quad \text{at} \leq 2.5\%\ H_2 \qquad (1)$$

where, A is a constant and $(^*R)_{H2}$ is the rate in pure H_2. This relationship is applicable at all temperatures and pressures. The reaction rate constant, K, is calculated from the relationship;

$$R = K A P^n \qquad (2)$$

where; R is the rate of reduction (% sec^{-1}), A is the specific surface area ($m^2.g.m^{-1}$) and P is the pressure of reducing gas at a given temperature (atm.) n is the slope of line which gives

the order of reaction. In H_2 and H_2/CO mixtures, the value of n is almost 1.0 (± 0.05). In pure CO, n= 1.23. The variation between the values of (K) and the gas composition is given in Figure 7.

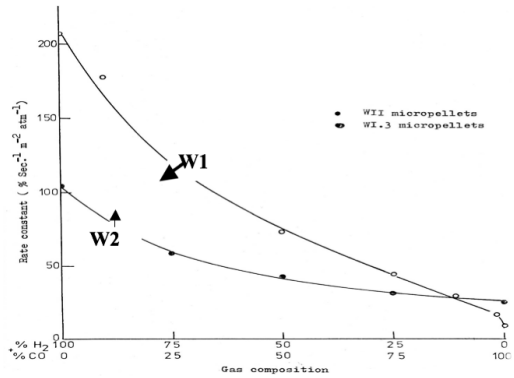

Figure 7: Variation between reduction rate constant (K) at initial reduction stages and gas composition at 1000°C

It shows that the gas composition has greatly influence on the values of (K) depend on the wüstite composition. In H_2, the value of (K) for W1 is two times higher than W1, while in CO, the value of (K) value of W2 is higher than that for W1. This is due to the presence of fayalite, which has a major influence of the rate of nucleation of iron.

The values of apparent activation energy values (E_a) for the reduction of W1 and W2 were computed from Arrhenius Equation [12]. Figure 8 shows the influence of gas composition on the (E_a) values calculated at 900-1100°C. It can be seen that the (E_a) values for W2 decreases gradually over the entire range of gases from 13.97 in H_2 to 6.78 kcal. mole-1 in CO. For W1, the (E_a) values increases from 12.86 in pure H_2 to 21.35 kcal.mole^{-1} in 97.5%CO-containing mixture beyond which, an abrupt increases in its value resulting 32.09 kcal.mole^{-1} in pure CO.

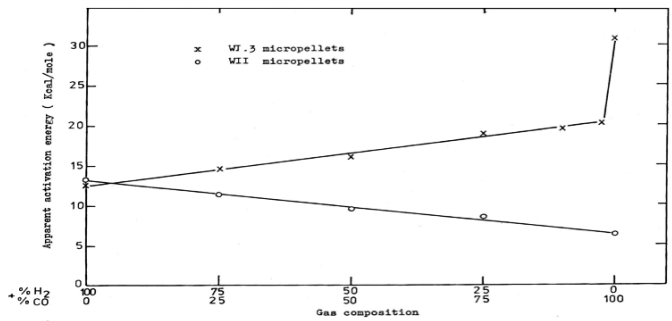

Figure 8: Influence of gas composition on the (E_a) values activation

The values of apparent activation energy at early stages, reveal several different rate controlling steps ranging from gaseous diffusion, interfacial chemical reaction and solid-state diffusion reactions. Under the present experimental reduction conditions, the reaction is most probably controlled by interfacial chemical at the initial stages since micropellets were used and the gas-boundary layer effect is eliminated. Also the solid state diffusion effect is negligible at the initial reduction stages. The wide scattering in (E_a) values (from

6.78 to 32.09 kcal.mole^{-1}) is resulted from the different pattern of nucleation and growths of iron on the oxide surface.

The SEM photomicrographs of 25% partially reduced W1 and W2 with H_2 and CO are given in Figures 9 (a, b, c).

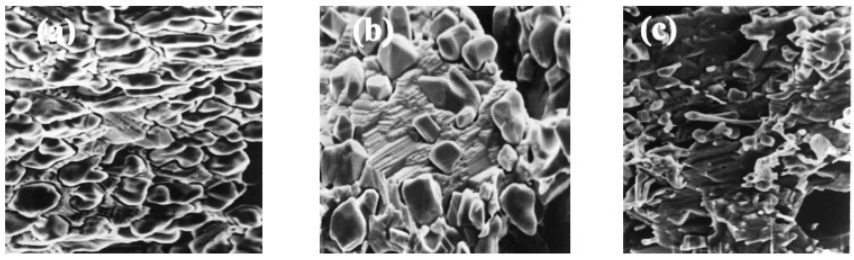

Figure 9: SEM photomicrographs of 25% reduced W1 (a,b) and W2 at 1000 °C

In W1, while the entire surface is covered by iron nuclei for the reduction with H_2 (Figure 9a), the surface is partially nucleated with iron in pure CO (Figure 9b). Therefore, a higher value of (E_a) is expected in CO reduction than in H_2 or H_2/CO mixtures. For W2 (Figure 9c), the surface is nucleated with iron nuclei, iron whiskers were formed through a combined effect of nucleation and growth on some active sites where fayalite ($2FeO.SiO_2$) is present. It has been reported that this phase is more easily reduced in CO than in H_2, since H_2 is unable to attack the regions where it is present [13].

The 75% reduced W1 and W2 at 1000°C in CO are shown in Figure 10 (a, b). The surface of W1 (Figure 10a) is partially nucleated with iron and the grains is disintegrated resulting in large numbers of smaller grains. The surface of W2 is surrounded by dense iron layer along the entire surface of grains. The mechanism of grain disintegration in W1 is attributed to the carbon deposition and the secondary reactions [12, 13] resulting CO_2 which entrapped in the grains till certain pressure (4-5 atm) after which the grains were disintegrated.

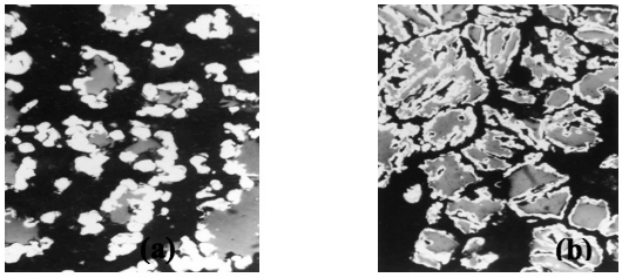

Figure 10: LM photomicrographs of (a)W1 and (b) W2 with CO at 1000°C

The influence of H_2 on the initiation of reduction of W1 was examined by carrying out the reduction at 1000°C in pure H_2 up to 25% extent to develop iron nuclei on the grain surface, then replced H_2 by CO till the end. The results obtained were compared with those in pure CO from the beginning, as shown in Figure 11. It can be clearly seen that the presence of H_2 is important at early stages to cover the oxide surface with iron nuclei which can be then enhancing the grain growth of these nuclei and speeding up the reduction process.

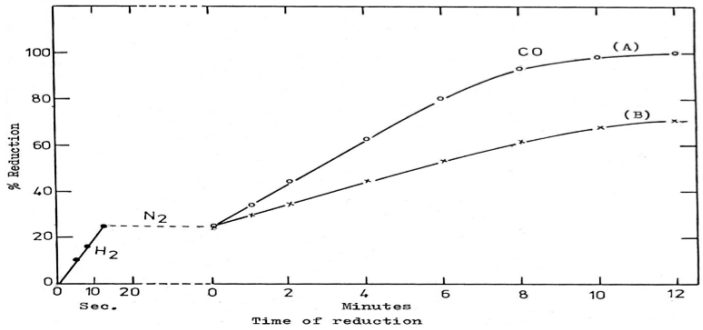

Figure 11: Reduction curves of W1 micropellets at 1000°C; Reduction with H_2 up to 25% extent then with pure CO. Reduction curve obtained in CO > 25% extent

Incubation Period, Nucleation and Grain Growth

An important feature of the reduction of W1 micropellets with CO at lower pressures is the presence of an incubation period. It is interesting to mention that about 220 seconds incubation period was detected in the reduction with CO at 0.1 P_{CO}. This period decreases with the increase in P_{CO}. On the other hand, this incubation period was not observed in the reduction with H_2 or H_2- containing gas mixtures. The formation of iron nuclei on the wüstite surface can take place by the removal of oxygen from oxide produces a local variation of the Fe/O ratio. After supersaturating is reached, the iron is separated out on the surface of wüstite in the form of nuclei. The iron formed is transported from the points where oxygen is removed to the points where nucleation and growth occur. This transport takes place through solid-state diffusion of iron along the surface. The number and distribution of iron nuclei depends upon the structural features of oxide (include lattice defects), the extent of grain boundaries and the foreign inclusions. The time required for the nucleation of metallic iron is quite dependent on the initial content of oxygen in the oxide. The quantity of oxygen removed in the nucleating period increases with increase of initial content of oxygen [15].

Mechanism of Reduction

The reduction with H_2 is characterized by the presence of initial rate constant up to certain extents depending on temperature and pressure, followed by a gradual decrease in the rate up to the end of reduction. The formed metallic iron is nucleated on the whole surface of wüstite grains. This indicates that the reduction reactions are not so complicated, since the (E_a) vales are in the interfacial chemical reaction range. The reactions by which wüstite is reduced to iron may proceed as follows;

$$(H_2)_g = (H_2)_{ads} \rightarrow 2H^+ + 2e^- \quad (3)$$

$$FeO \rightarrow Fe^{2+} + O^{2-} \quad (4)$$

$$2H^+ + O^{2-} \rightarrow (H_2O)_{ads} + (H_2O)_g \quad (5)$$

$$Fe^{2+} + 2e^- \rightarrow (Fe)_{nuclei} \quad (6)$$

On the other hand, the reduction rate with CO was much slower at initial stages than that in pure H_2 and H_2/CO gas mixtures at all temperatures and pressures. Moreover, the presence of incubation period is greatly retarded the reduction process. This evidence shows that the CO molecule is not directly reacted with FeO and it is most probably adsorbed on some active sites on the surface, then, reacted with wüstite to form intermediate carbonyl-like compound. After a while depending on temperature and P_{CO}, this compound dissociates to metallic iron and CO_2. The different reactions can be proposed as follows;

$$(CO)_{gas} \rightarrow (CO)_{ads} \tag{7}$$

$$FeO \rightarrow Fe^{2+} + O^{2-} \tag{8}$$

$$(CO)_{ads} + O^{2-} \rightarrow (CO_2)^{2-}_{ads} \tag{9}$$

$$n\,(CO_2)^{2-}_{ads} + m\,Fe^{2+} = [\,Fe_m\,(CO)_n\,]^* \rightarrow mFe + n(CO_2)_{ads} \tag{10}$$

$$(CO_2)_{ads} \rightarrow (CO_2)_{gas} \tag{11}$$

For the reduction with H_2/CO mixtures, it was found that the overall rate of reduction (Rmix.) is non-additive and can not be obtained using a simple equation in the form;

$$R_{mix} .= R_{CO} \,.\, X_{CO} + R_{H2} . X_{H2} \tag{12}$$

Where R_{CO} and R_{H2} are the rates in pure CO and H_2 at the pressure corresponding in the gas mixture and X_{CO} and X_{H2} are the mole fractions of CO and H_2 respectively. The presence of small amount of H_2 with CO greatly increases the rate of reduction due to the increase in the number of iron nuclei on the wüstite surface. The addition of small amount of CO to H_2 greatly lowered the reduction rate compared with pure H_2. This reduction mechanism is intensively discussed elsewhere [12, 13].

CONCLUSIONS

The highest rate of reduction was obtained in H_2 and decreases with the increase in CO content in the gas mixture. In pure CO, unlike in W2, the reduction of W1 showed an abrupt decrease in the rate which increases in presence of $\geq 2.5\%$ H_2. In pure H_2, the metallic iron was nucleated and covered the entire surface of W1 even at the initial reduction stages. In CO/H_2 gas mixtures, the reduction rate is non-additive. In pure CO at lower pressures, an incubation period was obtained at initial reduction stages for W1 which eliminated in presence of SiO_2. At later reduction stages, the grains were disintegrated due to the carbon deposition and CO_2 evolved at high pressure. A correlation between the overall rate of reduction in CO/H_2 gas mixture and the rate in pure gases was developed.

REFERENCES

Von Bogdandy, L. & Engell, H. J. (1971). *The Reduction of Iron Ores*. Springer Verlag. [1]

Oswald, J. (1981). BHP Tech. Bull., 25, pp.13. [2]

Panigraphy, S. C., Pverstraeten. & Dilewijns, J. (1984). Metall. Trans, 15B, pp. 23. [3]

El-Geassy, A. A. (1996). ISIJ. Int. 36 No. 11, pp. 1328. [4]

El-Geassy, A. A. (1996). ISIJ. Int. 36 ,No. 11, pp. 1344. [5]

El-Geassy, A. A. (1997). ISIJ. Int. 37 No. 9, pp. 844. [6]

Bahgat, M., Abdel-Halim, K. S., Nasr, M. I. & El-Geassy, A. A. (2007). Steel Research Int.78, p. 443. [7]

Bahgat, M., Abdel-Halim, K. S., Nasr, M. I. & El-Geassy, A. A. (2007). *Ironmaking – Steelmaking J*. 35, No. 3, p. 205. [8]

El-Geassy, A. A., Shehata, K. A.& Ezz, S. Y. (1977). J. Iron steel Int. Japan, p. 427. [9]

Bdurpre, M. El-Tabirou. & Gleitzer, C. (1988). Metall. Trans., 19B, p. 479. [10]

Turkdogan, E. T. & Vinters, J. V. (1974). Metall. Trans 5B p.11. [11]

El-Geassy, A. A. (1985). J. Iron steel Int. Japan, 25 p. 451. [12]

El-Geassy, A. A. (1985). J. Iron steel Int. Japan, 25 p. 1037 [13]

Sadrehashemi, F. (1977). *The Reduction of Hematite to Magnetite in H_2-H_2O Mixture*, Ph.D. Thesis, London Univ. [14]

Shewmon, P. G. (1969). *Transformations in Metals*. McGraw-Hill, New York. [15]